**Agata Kukuła-Kurzyniec[1]\*, Jan Dutkiewicz[1], Piotr Bobrowski[1], Wojciech Wajda[1]
Anna Góral[1], Patrick Ochin[2], Loïc Perrière[2]**

[1] Institute of Metallurgy and Materials Science, PAS, ul. Reymonta 25, 30-059 Krakow, Poland
[2] ICMPE, CNRS UMR 7182, 2-8 rue Henri Dunant, 94320 Thiais, France
\* Corresponding author: a.kukula.kurzyniec@interia.eu

# STRENGTHENING OF ALUMINIUM BASED COMPOSITES WITH AMORPHOUS METALLIC OR Al$_2$O$_3$ PARTICLES

Aluminium alloy based composites were prepared by hot pressing in a vacuum in order to study the strengthening effect of an amorphous phase addition in the form of ball milled powder from melt spun ribbons of the Al$_{73}$Si$_5$Ni$_7$Cu$_8$Zr$_7$ (at.%) alloy. For comparison, a composite with a strengthening ceramic Al$_2$O$_3$ phase was hot pressed under the same conditions. DSC measurements allowed the authors to determine the start of the crystallization process of the amorphous ribbons at 240ºC. The presence of the majority of the amorphous phase in the melt spun ribbons was additionally confirmed by the X-ray diffraction technique which also revealed the presence of an α-Al solid solution and some peaks of intermetallic phases. SEM studies showed homogenous distribution of the strengthening particles in both kinds of composites and confirmed the existence of α-Al and some intermetallic crystallites inside the metallic amorphous particles. The hardness of all the prepared composites was comparable and amounted to approximately 50 HV1 for those with the Al matrix and 120 HV1 for the ones with the 2618A alloy matrix. The composites have shown a higher yield stress than the hot pressed aluminium or 2618A alloy. SEM studies of the cracks after compression tests revealed that the interfaces between the strengthening phase and matrix in metallic amorphous powder-Al /2618A alloy composites show a different character of the interface between the ceramic particles and the Al matrix. Therefore in the composite with the Al$_2$O$_3$ particles, cracks have the tendency to propagate at the interfaces with the matrix more often than in amorphous/Al composites.

Keywords: Al-based-amorphous composites, Al-based-Al$_2$O$_3$ composites, melt spinning, powder hot pressing, compression tests

## UMOCNIENIE KOMPOZYTÓW NA OSNOWIE ALUMINIUM POPRZEZ DODATEK METALICZNEJ FAZY AMORFICZNEJ LUB CZĄSTEK Al$_2$O$_3$

W artykule opisano badania dotyczące struktury i właściwości kompozytów na osnowie aluminium i jego stopu - 2618A, wykonanych metodą prasowania na gorąco w próżni. Fazę umacniającą stanowił 10% dodatek proszku o składzie Al$_{73}$Si$_5$Ni$_7$Cu$_8$Zr$_7$ (% at.), otrzymany w wyniku mielenia kulowego metalicznych taśm amorficznych odlanych na wirujący walec (melt spinning). W celu porównawczym w tych samych warunkach sprasowano również kompozyt o osnowie Al, w którym fazę umacniającą stanowił 10% dodatek cząstek ceramicznych - Al$_2$O$_3$. Metodą mikrokalorymetrii różnicowej (DSC) określono temperaturę początku krystalizacji taśm amorficznych na około 240ºC. Techniką dyfrakcji rentgenowskiej (XRD) potwierdzono obecność znacznego udziału struktury szklistej zarówno w odlanych, jak i sproszkowanych taśmach, a także stwierdzono niewielki udział roztworu α-Al oraz faz międzymetalicznych. Badania strukturalne wykonane metodą skaningowej mikroskopii elektronowej (SEM) wykazały równomierne rozmieszczenie cząstek faz umacniających w obu rodzajach kompozytów, a w przypadku cząstek taśm amorficznych potwierdzono obecność w ich wnętrzu krystalitów roztworu α-Al i faz międzymetalicznych. Twardość wszystkich przygotowanych kompozytów była porównywalna i wynosiła około 50 HV1 dla kompozytów o osnowie Al oraz 120 HV1 dla materiałów na bazie stopu 2618A. Obserwacja SEM mikrostruktury próbek kompozytowych po testach ściskania pozwoliła zauważyć inny charakter granicy rozdziału cząstek fazy umacniającej i osnowy w przypadku zastosowania cząstek taśmy Al$_{73}$Si$_5$Ni$_7$Cu$_8$Zr$_7$, co wpływa na odmienny przebieg drogi propagacji pęknięć niż w przypadku proszku Al$_2$O$_3$, gdzie występuje słabsze połączenie w granicy osnowa-cząstki wzmacniające. W przypadku zastosowania ceramicznej fazy umacniającej kompozyt wykazuje tendencję do propagacji pęknięć po granicach wprowadzonych cząstek.

Słowa kluczowe: kompozyty na osnowie Al umacniane fazą amorficzną, kompozyty metaliczno-ceramiczne, odlewanie na wirujący walec, prasowanie proszków na gorąco, badania wytrzymałości metodą ściskania

## INTRODUCTION

Aluminium based composites strengthened with ceramic phases are now being widely used due to their good mechanical properties combining high strength and good properties at elevated temperatures [1-3]. The flow stress of the Al-base composite material at any particular strain rate or temperature increases with an

increasing reinforcement content, increasing strain rate, and decreasing temperature [1, 2]. The composites strengthened with $TiB_2$ and $Al_2O_3$ particles exhibit a relatively stable cyclic response, however, intermetallic $Al_3Ti$ blocks reduce the fatigue life [3].

Recently, amorphous alloys have been used as a component of metal based composites [4-6]. Either copper or nickel was used as the matrix of the composites [4, 5] allowing the authors to obtain high strength and plasticity due to a unique combination of the high tensile strength of the amorphous metallic alloys, good resistance to wear and corrosion (due to the absence of grain boundaries) and high elasticity [7-9]. The copper based composite was obtained by multiple rolling and joining of amorphous ribbon and copper [4], while the nickel based one was obtained by sintering Ni covered amorphous powders [5]. The addition of copper to the amorphous powder allowed the authors to substantially increase the plasticity of the amorphous phase [6]. Amorphous metals derive their strength directly from their non-crystalline structure, which exhibits a different mechanism of deformation with a propagation of narrow deformation bands where fine crystalline nuclei are observed [7]. A tensile strength exceeding 1200 MPa was reported, which is twice as high as for conventional commercial aluminium alloys [7, 8]. Al-based glasses are characterized by low densities of about $3.2 \div 3.7$ g/cm$^3$ which indicates their potential applications in transportation. The first formation of the amorphous single phase in Al-based alloys containing more than 50 at.% Al was found in 1981 for Al-Fe-B and Al-Co-B ternary alloys [9] but they did not attract much attention due to their high brittleness. The majority of compositions of aluminium based metallic glasses include rare earth (RE) metals, usually with an Ni addition [9], however, sometimes also with an Si addition [10, 11].

The glass forming ability in Al-Si-Ni based alloys with other metallic additions was reported as very good by Cieślak in his PhD thesis [12] and Kaikai Song et al [13]. The alloys yielded almost complete amorphization in the melt spun state. In the present paper, an Al-Si-Ni based alloy without RE additions was chosen with a base composition of the ternary eutectic AlNiSi after the phase diagram in [14], however, amorphization of hypereutectic alloys was also investigated in [15]. The composition of the melt spun Al-Ni-Si based alloy was chosen to improve the glass forming ability (GFA). The factors that influence GFA include atomic radius differences, enthalpy of mixing, maximum extended solid solubility [1, 16] and the difference in the atomic radius of the components. These conditions are fulfilled for the eutectic Al-Ni-Si composition and can be even extended in alloys with zirconium and copper additions, due to the reported positive effect of Zr on the amorphization behaviour of Al based alloys [7, 15, 16].

In the present paper, an aluminium based amorphous alloy in the form of ball milled, refined melt spun ribbon was used as a strengthening addition to an aluminium matrix to obtain bulk composites in order to con-

tribute to basic research similarly as in [4, 5]. The mechanical properties were compared to those of Al-Al$_2$O$_3$ composites prepared in a similar way.

## EXPERIMENTAL PROCEDURE

### Materials

Two types of composites with an aluminium or 2618A aluminium alloy matrix were investigated - one with the addition of amorphous metallic particles of $Al_{73}Si_5Ni_7Cu_8Zr_7$ (at.%) alloy as a strengthening phase and, as a reference, another with $Al_2O_3$ - ceramic powder with a mean particle size of 60 μm. The amorphous structure in the $Al_{73}Si_5Ni_7Cu_8Zr_7$ alloy was obtained by the melt spinning method. The initial ingots were prepared by arc-melting in a purified, Zr-gettered argon atmosphere from high purity elements (99.9 wt.% and more) and then subjected to the melt spinning process. The alloys were placed in quartz crucibles in an enclosed chamber and then ejected using He overpressure of 0.2 MPa at a linear speed of a copper wheel of 20 m/s. The ribbons were subsequently milled in a high energy planetary ball mill "Pulverisette 5" at 200 rpm under a protective argon atmosphere using steel bearing balls. The process lasted for 6 hours and each 15 minutes of milling was followed by a 45-minute pause for cooling down to avoid overheating of the ribbons. The obtained powder was blended with an aluminium or aluminium 2618A alloy in the compositions of: 90% Al + 10% $Al_{73}Si_5Ni_7Cu_8Zr_7$ and 90% 2618A + 10% $Al_{73}Si_5Ni_7Cu_8Zr_7$. The aluminium based powder of alloy 2618A consisted of additions of: 2.42% Cu, 1.55% Mg, 1.29% Ni, 1.01% Fe, 0.54% Zr and < 0.5% of Si, Zn, Ti, Mn. The composition of 90% Al + 10% $Al_2O_3$ was prepared to compare its mechanical properties with previously mentioned amorphous-Al based compositions. All three blends were compacted into discs of a 20 mm diameter by uniaxial hot pressing under the vacuum of $10^{-2}$ bar at the temperature of 380°C and the pressure of 600 MPa applied for 10 minutes (similarily as in [17, 18]). Samples cut from the composites were subjected to compression tests and subsequently examined by SEM methods.

### Methods

The structure and composition were studied using scanning electron microscopes - Philips XL 30 and Quanta 3D FEG. X-ray diffraction was performed using a Philips PW 1710 diffractometer with Co Kα radiation. Compression tests were carried out with an Instron 3382 tensile machine with a rate of $10^{-3}$ s$^{-1}$, the hardness was checked with a Zwick ZHU 250 instrument and microhardness tests were performed with a CSM Instruments Microhardness Tester with a load of 0.1 N. Differential Scanning Calorimetry (DSC) studies with a Netzsch Pegasus 404 - F1 thermal analyser allowed the authors to observe the thermal effects in the alloy

and determine the crystallization temperature in the partially amorphous ribbon. Continuous heating of the samples was performed at a rate of 20 K/min. The studies were performed in accredited research laboratories.

## RESULTS AND DISCUSSION

Figure 1 presents the X-ray diffraction pattern from the melt spun ribbon of Al$_{73}$Si$_5$Ni$_7$Cu$_8$Zr$_7$. The broad halo indicates a large amount of amorphous structure, however, some additional peaks appear which indicate the formation of crystalline phases like an α−Al solid solution and intermetallic compounds like AlNi and Zr$_2$Si.
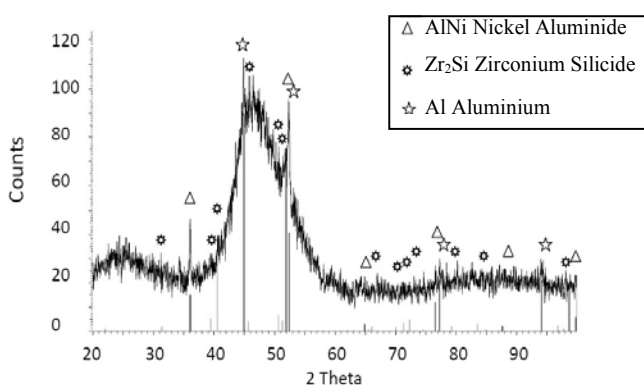


Fig. 1. X-ray diffraction pattern from melt spun ribbon of Al$_{73}$Si$_5$Ni$_7$Cu$_8$Zr$_7$ composition

Rys. 1. Dyfraktogram rentgenowski uzyskany dla taśmy o składzie Al$_{73}$Si$_5$Ni$_7$Cu$_8$Zr$_7$ wytworzonej metodą melt spinning

Amorphization of the ribbon was additionally confirmed by DSC study, shown in Figure 2. The set of exothermal peaks indicates the multistage crystallization process which starts at the temperature of 243$^o$C. The other maxima occur at the temperatures of 260, 305, 342 and 425$^o$C and correspond to the crystallization of various phases. No glass transition effect was observed as also reported for other aluminium alloys [12], however, from the increase in the crystallization temperature comparing to other Al-Si-Ni based alloys [19], one can judge that the $\Delta T_c$ ($T_L - T_x$) increases with the addition of Cu and Zr to the composition and therefore also glass forming ability with the addition of quaternary and quinternary elements [7].

To determine the morphology and chemical composition of the crystalline inclusions, SEM techniques were applied. The microstructure with crystallites in the melt spun ribbon of the Al$_{73}$Si$_5$Ni$_7$Cu$_8$Zr$_7$ composition is presented in Figure 3. The elongated crystallites seen as brighter particles in the grey matrix are located near the surface, since the bottom part of the ribbon at the copper wheel side with a higher cooling rate does not show crystalline particles.

The results of the microanalysis indicate the presence of an Al$_3$Zr phase with a small amount of some other solute elements, considering the fact that the EDS

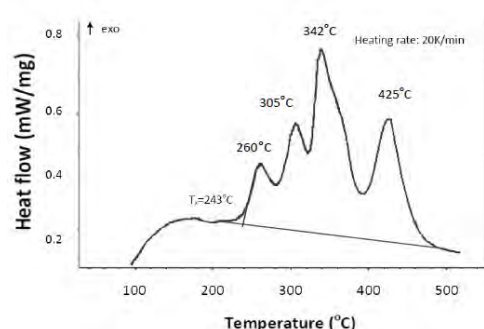analysis of the inclusions is modified by the radiation of the matrix lying beneath them.



Fig. 2. DSC curve obtained from Al$_{73}$Si$_5$Ni$_7$Cu$_8$Zr$_7$ ribbon

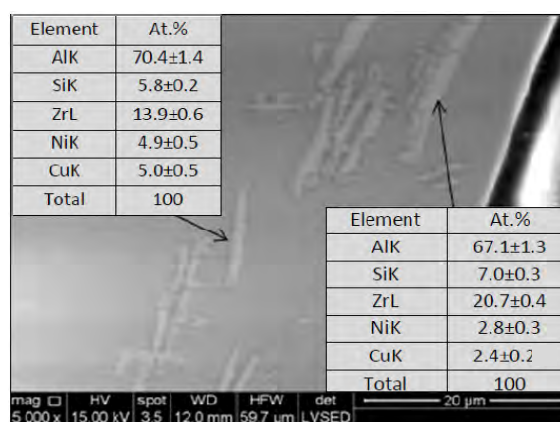Rys. 2. Krzywa DSC otrzymana dla taśmy ze stopu Al$_{73}$Si$_5$Ni$_7$Cu$_8$Zr$_7$



Fig. 3. SEM microstructure with EDS analysis of melt spun ribbon (Al$_{73}$Si$_5$Ni$_7$Cu$_8$Zr$_7$) showing crystalline inclusions in amorphous matrix

Rys. 3. Mikrostruktura SEM wraz z analizami EDS taśmy Al$_{73}$Si$_5$Ni$_7$Cu$_8$Zr$_7$ odlanej techniką melt spinning, ukazująca krystaliczne wydzielenia w amorficznej osnowie

The melt spun ribbons with a predominantly amorphous structure were subsequently subjected to the ball milling process for 6 hours. The X-ray diffraction pattern of the powdered ribbon is presented in Figure 4.
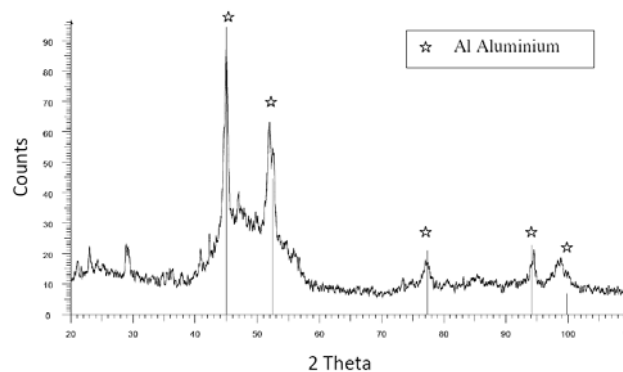


Fig. 4. X-ray diffraction pattern from milled ribbon of Al$_{73}$Si$_5$Ni$_7$Cu$_8$Zr$_7$ composition

Rys. 4. Dyfraktogram rentgenowski uzyskany dla mielonej taśmy o składzie Al$_{73}$Si$_5$Ni$_7$Cu$_8$Zr$_7$

One can see that the XRD pattern still shows a broadened halo coming from the amorphous part of the particles and several clear peaks of the α-Al solid solution which means that the milling process did not cause significant crystallization of the structure. Some peaks coming most probably from intermetallic phases could not be indexed due to insufficient information. The powdered ribbon was blended with two types of matrixes - Al and aluminium alloy - 2618A and then subjected to the hot pressing process. The SEM microstructure of the 90% Al + 10% $Al_{73}Si_5Ni_7Cu_8Zr_7$ composite is presented in Figure 5. It shows refined ribbon particles with some crystalline inclusions, distributed rather uniformly in the aluminium matrix of the composite.
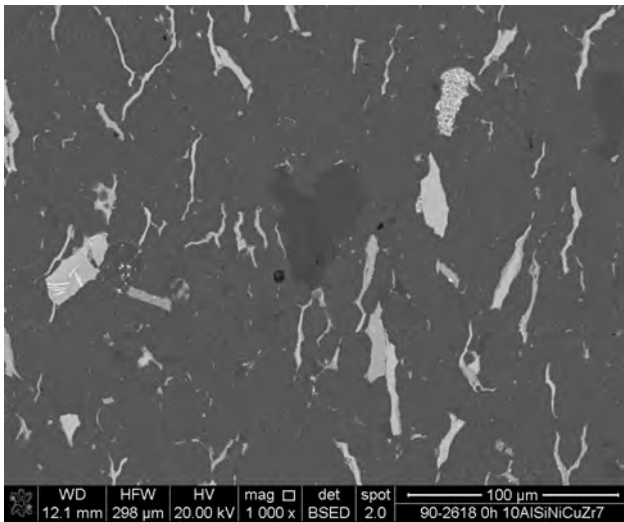


Fig. 5. SEM microstructure of 90% Al + 10% $Al_{73}Si_5Ni_7Cu_8Zr_7$ composite showing refined ribbon particles with some crystalline inclusions and Al matrix

Rys. 5. Mikrostruktura SEM kompozytu 90% Al + 10% $Al_{73}Si_5Ni_7Cu_8Zr_7$ przedstawiająca rozdrobnione cząstki taśmy wraz z wydzieleniami krystalicznymi w osnowie z Al

The compression test curves of all the investigated materials are presented in Figure 6. The hot pressed aluminium showed the lowest yield strength - about 110 MPa and yielded a deformation of about 40% while the composite strengthened with $Al_2O_3$ or with amorphous particles showed a higher yield stress near 130 MPa. However, the ceramic phase addition significantly lowered the plasticity of the composite. The composite consisting of 90% 2618A alloy strengthened with a 10% $Al_{73}Si_5Ni_7Cu_8Zr_7$ amorphous phase shows a higher yield stress of 250 MPa than the hot pressed alloy (220 MPa), however, the latter reached a higher compression strength of about 500 MPa at a plastic deformation of 70%.

Figure 7 presents the SEM micrographs of cracks arising in the compression test in two types of composites - with metallic amorphous and ceramic particles in an Al matrix. As can be seen, the cracks in the amorphous - Al composite do not have the tendency to propagate in the interfaces between the strengthening particles and matrix. The phenomena can be explained with the diffusive character of the interfaces causing better adhesion which is not the case in the composite with the $Al_2O_3$ particles where the cracks have the tendency to propagate on the interfaces with the matrix. The propagation of cracks in the composite based on the 2618A alloy is similar to the one with the Al matrix.
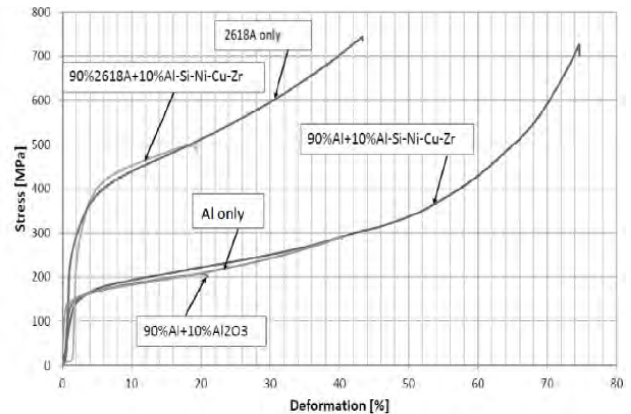


Fig. 6. Compression curves of hot pressed Al and 2618A alloy and composites with $Al_{73}Si_5Ni_7Cu_8Zr_7$ and $Al_2O_3$ additions used as reinforcing phases

Rys. 6. Krzywe z prób ściskania prasowanego na gorąco Al oraz stopu 2618A oraz kompozytów z dodatkami $Al_{73}Si_5Ni_7Cu_8Zr_7$ oraz $Al_2O_3$ zastosowanymi jako fazy umacniające
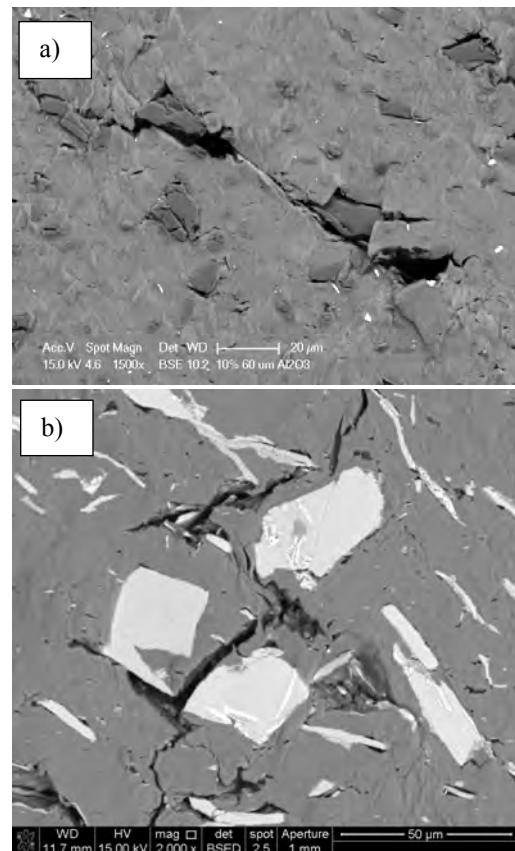


Fig. 7. SEM micrographs of composites deformed in compression test: a) 90% Al+10% $Al_{73}Si_5Ni_7Cu_8Zr_7$, b) 90% Al+10% $Al_2O_3$ (60 μm)

Rys. 7. Mikrofotografie SEM kompozytów po deformacji w próbie ściskania: a) 90% Al+10% $Al_{73}Si_5Ni_7Cu_8Zr_7$, b) 90% Al+ +10% $Al_2O_3$ (60 μm)

The hardness of the investigated composites is as follows:

| | |
|---|---|
| 90% Al+10% Al$_2$O$_3$ | – 48 HV1, |
| 90% Al+10% Al$_{73}$Si$_5$Ni$_7$Cu$_8$Zr$_7$ | – 52 HV1, |
| 90% 2618A+10% Al$_{73}$Si$_5$Ni$_7$Cu$_8$Zr$_7$ | – 121 HV1 |

(pressed Al - 54 HV1, pressed 2618A – 112 HV1).

The hardness of the composites with the Al matrix was comparable and amounted to nearly 50 HV1, the hardness of the one with the 2618A matrix was slightly higher than for the 2618A alloy. The microhardness tests (Fig. 8) showed a high microhardness (over 700 HV 0.01) of the amorphous particles and therefore it can be assumed that a higher than 10% addition of amorphous particles to the composite could increase the hardness value.
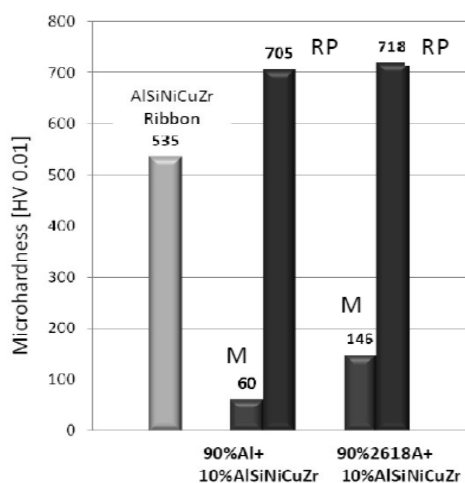


Fig. 8. Microhardness histogram  determined for melt spun ribbon and phases in composites:  90% Al+10% Al$_{73}$Si$_5$Ni$_7$Cu$_8$Zr$_7$  and 90% 2618A+10% Al$_{73}$Si$_5$Ni$_7$Cu$_8$Zr$_7$; respectively: RP - reinforcing particles, M - matrix

Rys. 8. Histogram przedstawiający mikrotwardość określoną dla taśmy oraz faz w kompozytach: 90% Al+10% Al$_{73}$Si$_5$Ni$_7$Cu$_8$Zr$_7$ oraz 90% 2618A+10% Al$_{73}$Si$_5$Ni$_7$Cu$_8$Zr$_7$; odpowiednio: RP - cząstki umacniające, M - osnowa

The compression strength of the aluminium based composites was much lower than that observed in the Ni/amorphous [5] or in Cu/amorphous ones [4], however, in those papers the amount of amorphous phase was much higher, approaching 70% in [5] or even 80% in [4] and the yield strength was higher or similar to the 2618A based composite at a lower amorphous phase content.

## CONCLUSIONS

1) The compression strength of Al based/amorphous strengthening phase composites does not increase significantly due to the 10% addition of amorphous phase, however, a similar strengthening effect is obtained as for the addition of ceramic phase. The addition of an amorphous phase does not cause a decrease in the plastic deformation during the compression test as in the case of the Al$_2$O$_3$ strengthened composite. It is most probably caused by the diffusive character of the interface which causes better adhesion of the amorphous particles with the matrix, where only a few cracks were observed at the amorphous/Al interfaces, contrary to the Al$_2$O$_3$ strengthened composite. A higher fraction than 10 wt.% amorphous phase is needed to strengthen the composites as much as in the other works.

2) The milled and sieved melt spun ribbon of the Al$_{73}$Si$_5$Ni$_7$Cu$_8$Zr$_7$ aluminium alloy can be used as the strengthening phase in the composites as its amorphous structure does not undergo significant crystallization during hot pressing at 380$^o$C. XRD of the ball milled ribbon showed the coexistence of an amorphous structure and some amount of an α-Al solid solution and intermetallic phases which only slightly lower the hardness of the ribbons. The DSC studies showed that the crystallization in the investigated ribbons proceeds as a multistage process manifested by a sequence of exothermal peaks appearing during  continuous heating with  a start near the temperature of 243$^o$C.

## Acknowledgements

## REFERENCES

[1] Kaczmar J.W., Pietrzak K., Włosiński W., The production and application of metal matrix composite materials, Materials J. Proc. Technol. 2000, 106, 58-67.

[2] Issam S. Jalham, A comparative study of some network approaches to predict the effect of the reinforcement content on the hot strength of Al-base composites, J. Materials Proc. Technol. 2005, 166, 392-397.

[3] Tjong S.C., Wang G.S., Mai Y.W., Low-cycle fatigue behavior of Al-based composites containing in situ TiB$_2$, Al$_2$O$_3$ and Al$_3$Ti reinforcements, Mater. Sci. Eng. A 2003, 358, 99-106.

[4] Lee M.H., Park J.S., Kim J.-H., Kim W.T., Kim D.H., Synthesis of bulk amorphous alloys and composites by warm rolling process, Materials Letters 2005, 59, 1042-1045.

[5] Lee J.H., Park E.S., Lee J.C., Huh M.Y., Kim H.J., Bae J.C., In situ microfracture observation of Cu-based amorphous alloy matrix composites containing copper or brass particles, Mater. Sci. Eng. A 2009, 508, 15-22.

[6] Chang-Young Son, Chang Kyu Kim, Seung Yong Shin, Sunghak Lee, Microstructure and mechanical properties of Cu-base amorphous alloy matrix composites consolidated by spark plasma sintering, Mater. Sci. Eng. A 2007, 449-451, 924-928.

[7] Suryanarayana C., Inoue A., Bulk Metallic Glasses, CRC Press, Boca Raton 2012.

[8] Gogebakan M., Warren P.J., Cantor B., Crystallization behavior of amorphous Al$_{85}$Y$_{11}$Ni$_4$ alloy, Mater. Sci. Eng. A 1997, 226-228, 168-172.

[9] A. Inoue, Amorphous, nanoquasicrystalline and nanocrystalline alloys in Al-based systems, Prog. Mater. Sci. 1998, 43, 365-520.

[10] Lee T.H., Kawamura Y., Inoue A., Cho S.S., Masumoto T., Mechanical properties of rapidly solidified Al-Si-Ni-Ce P/M alloys, Scr. Metall. 1997, 36, 475.

[11] Latuch J., Cieślak G., Kulik T., Fabrication and structure of bulk nanocrystalline Al-Si-Ni-mishmetal alloys, Alloys J., Comp. 2007, 434-435, 272-274.

[12] Cieślak G., Wytwarzanie nanokrystalicznych stopów z układu Al-Si-Ni-Mm (miszmetal). PhD thesis, Politechnika Warszawska, Warszawa 2012.

[13] Kaikai Song, Xiufang Bian, Jing Guo, Shenghai Wang, Bao'an Sun, Xuelian Li, Caidong Wang, Effects of Ce and Mm additions on the glass forming ability of Al-Ni-Si metallic glass alloys, J. Alloys Comp. 2007, 440, L8-L12.

[14] Villars P., Prince A., Okamoto H., Handbook of Ternary Alloy Phase Diagrams, ASM Int., Ohio 1995, 4167.

[15] McKay B.J., Cizek P., Schumacher P., O'Reilly K.A.Q., Heterogeneous nucleation in an Al-Ni-Si alloy studied using a metallic glass technique, Mater. Sci. Eng. A, 2001, 304-306, 240-244.

[16] Wang L., Ma L., Kimura H., Inoue A., Amorphous forming ability and mechanical properties of rapidly solidified Al-Zr-LTM (LTM=Fe, Co, Ni and Cu) alloys, Materials Letters 2002, 52, 47-52.

[17] Dutkiewicz J., Maziarz W., Lityńska-Dobrzyńska L., Góral A., Kukuła A., Kanciruk A., Kompozyty nanokrystaliczne na osnowie stopu aluminium 6061 z dodatkami fazy ceramicznej α-Al$_2$O$_3$, Kompozyty (Composites) 2010, 10, 1, 76-80.

[18] Dutkiewicz J., Kukuła-Kurzyniec A., Lityńska-Dobrzyńska L., Ochin P., The structure and properties of composites based on silver and aluminium alloys strengthened with amorphous phase, Composites Theory and Practice 2012, 12,1, 44-49.

[19] Kukuła-Kurzyniec A., Dutkiewicz J., Ochin P., Perrière L., Dłużewski P., Góral A., Amorphous - nanocrystalline structure and properties of melt spun Al-Si-Ni based alloys, Archives of Metallurgy and Materials (2/2013, in print).